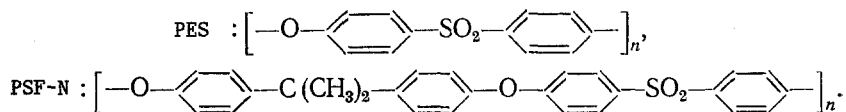


Results of a study of polysulfone thermophysical properties and their relationship to relaxation processes are presented.

At the present time, among the polymer materials used for construction purposes, polysulfones are becoming ever more significant [1]. This class of thermostable polymers is distinguished by high chemical stability, strength at elevated temperatures, and other unique properties [1]. Despite these facts, the physical properties of these polymers have remained practically unstudied. The authors have performed a study of thermophysical characteristics (thermal conductivity coefficient and specific heat) of polysulfones of various chemical chain structures. It has been shown in a number of studies [2, 3] that polymer properties are affected significantly by relaxation processes and molecular mobility of their structural elements. Therefore it is of indisputable interest to establish the basic principles relating thermophysical properties and relaxation processes in polymers [4].

The study performed used mutually independent and complementary techniques: a) dynamic thermophysical techniques for study of thermal conductivity ( $\lambda$ ), specific heat ( $C_p$ ), and linear expansion ( $\alpha$ ); b) dynamic mechanical free and constrained resonant oscillations, from which the tangent of the mechanical loss angle was determined [2, 3]. At a confidence level of  $\alpha = 0.95$  the accuracy of the methods were respectively, for  $\lambda$  6%,  $C_p$  2%,  $\alpha$  0.2%,  $\tan \delta$  6.0%. The objects of study were two types of polysulfones, differing in the chemical structure of their molecular chains: polyethersulfone (PES) and polysulfone N (PSF-N) with molecular mass of  $5 \cdot 10^4$ :



The thermal strength studies performed on these polysulfones revealed their high thermal stability. Thus, for PES the temperature at which intense destruction commenced was 763 K, and for PSF-N, 748 K. In all probability the high thermal stability of polysulfones is insured by formation of free radicals upon splitting of the sulfone group, which leads to cross-linking of the polymer in the early stages of thermal destruction.

In regions of thawing of molecular mobility of various elements of the polymer dynamic structure a change occurs in the temperature coefficient of the characteristics studied, which is expressed in the form of discontinuities in the temperature curves (Fig. 1). As is evident from the figure, thermophysical characteristics studied are sensitive to various degrees to "thawing" of thermal motion of structural elements. In the temperature dependence of the thermal conductivity coefficient there are visible two ranges in which the temperature coefficient changes, which indicate changes in the conditions for heat transport through the spectrum. The quantity most sensitive to change in the intensity of molecular motion is the specific heat. There exist several "discontinuities" in the temperature dependence of specific heat (Fig. 1). At temperatures of 483 K for PES and 449 K for PSF-N there occurs within the vitrification region a transition of the polymer from the vitreous to a highly elastic state. The discontinuities in thermal conductivity comprise 200 and 260 J/(kg·K) for PES and PSF-N respectively. A higher value of vitrification temperature and smaller discontinuity in specific heat indicates more intense intermolecular interaction in PES as compared to PSF-N. Apparently the decrease in intermolecular action in PSF-N occurs as a result of appearance within the macromolecule of an isopropylidene group.

A. M. Gor'kii State Pedagogic Institute, Kiev. Translated from *Inzhenerno-Fizicheskii Zhurnal*, Vol. 53, No. 6, pp. 942-949, December, 1987. Original article submitted June 9, 1986.

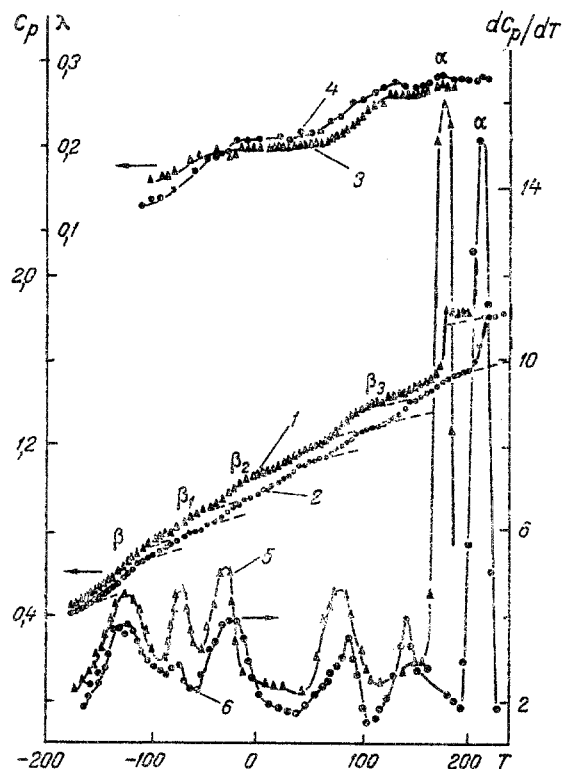


Fig. 1. Temperature dependence of specific heat  $C_p$  (1, 2); thermal conductivity coefficient  $\lambda$  (3, 4) and derivative  $dC_p/dT$  (5, 6) for polymers PSF-N (1, 3, 5) and PES (2, 4, 6).  $C_p$ , kJ/(kg·K);  $\lambda$ , W/(m·K);  $T$ , °C.

The more intense intermolecular effect is confirmed by the larger value of PES density (1371.2) as compared to PSF-N (1242.4 kg/m<sup>3</sup>).

The lower absolute values of PES specific heat over the entire temperature interval studied also indicate lower intensity of molecular motion. The higher value of the shear modulus  $G'$  (Fig. 2, curves 3, 4) for PES is determined by more intense molecular interaction. On this basis, the higher absolute values of the thermal conductivity coefficient of PES become understandable as well. The calculated phonon free path length ( $\langle \ell \rangle = 3\lambda/\rho C_p v_{SO}$ ) using the experimental data obtained herein ( $v_{SO} = 2350$  m/sec at 293 K) is equal to 1.95 Å for PES and 1.80 Å for PSF-N. This also indicates that phonon scattering in the more densely packed polymer with intense molecular interaction occurs at greater lengths, and as a result, energy transfer is accomplished more intensely. The character of the temperature dependence of thermal conductivity, namely, the increase with temperature, is controlled by both the intensity of thermal motion, and the change in intermolecular interaction. The latter factor completely determines the temperature dependence of the dynamic shear modulus  $G'$  (Fig. 2). To establish the relationship between thermophysical properties and relaxation processes internal stress spectra were obtained. Results for one of the frequencies are shown in Fig. 2 (curves 1, 2).

The results were proposed by relaxation spectrometry methods [3, 5] using data available in [6-8].

In the internal stress spectra of Fig. 2 relaxation transitions (in the regions where molecular mobility appears) appear as individual maxima or "spikes" in the temperature dependence of specific heat, so-called structural relaxation [5].

To each of these relaxation maxima there corresponds a relaxation transition with satisfaction of the condition

$$\omega\tau_i = 2\pi\nu\tau_i = c_i, \quad (1)$$

where for polymers the constant  $c_i \approx 1-10$ , depending on the type of relaxation transition [9];  $\omega$  is the circular frequency;  $\nu$  is the linear frequency (indicated in Fig. 2 for the

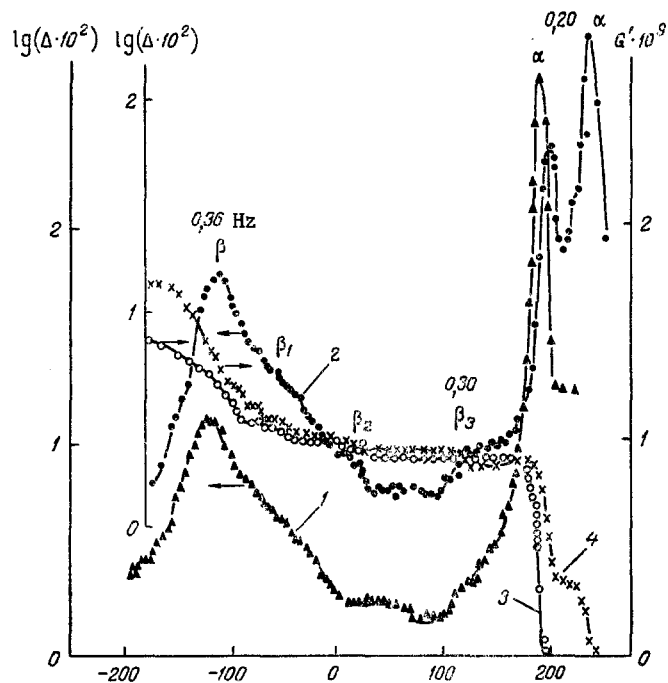


Fig. 2. Temperature dependence of the logarithm of the damping decrement for polymers PSF-N (1), PES (2) and modulus  $G'$  of PSF-N (3), PES (4),  $G'$ ,  $N/m^2$ .

observed relaxation transitions);  $\tau_i$  is the relaxation time of relaxation transition 1.

All transitions noted in the spectrum are beyond the limits of experimental uncertainty. To obtain a more precise determination of temperature at which relaxation transitions appear, the curve of the temperature dependence of specific heat, presmoothed with consideration of experimental uncertainty, was differentiated numerically. Results of this differentiation are shown in Fig. 1 (curves 5, 6). We see that the curve  $dC_p/dT$  formally reflects the appearance of molecular mobility processes. The temperatures of relaxation transitions correspond to maxima in the function  $dC_p/dT$ . The conditions of appearance of a relaxation transition for structural relaxation for processes, the activation energy of which is temperature-independent have the form form [3]:

$$w\tau_i = c_0 = kT_i^2/U_i, \quad (2)$$

where  $w$  is the heating rate;  $k$  is Boltzmann's constant;  $U_i$  is the activation energy of the  $i$ -th relaxation transition. To determine values of the basic relaxation parameters of the preexponential coefficients  $B_i$  of the Boltzmann-Arrhenius equation for the  $i$ -th relaxation transition we make use of Eq. (1) and the Boltzmann-Arrhenius equation:  $\tau = B_i \exp(U_i/kT)$ . Simultaneous solution gives

$$\frac{1}{T_i} = \frac{2,3k}{U_i} \lg \frac{c_i}{2\pi B_i} - \frac{2,3k}{U_i} \lg v. \quad (3)$$

For the majority of fine-scale relaxation transitions in polymers the dependence of  $1/T_i$  on  $\log v$  is linear. Figure 3 shows processing results for the most intense low-temperature transition of the polymers studied, which we have denoted by  $\beta$ . The graphs also show points obtained by processing the internal friction spectra of other authors [6-8]. Data from this analysis of PES and PSF-N relaxation transitions are presented in Table 1. To identify relaxation processes obtained from thermophysical measurements, it is necessary to calculate the equivalent mechanical frequency  $\nu_{eq}$ , corresponding to the heating rate  $w$  [3]. In Eqs. (1) and (2) the value of the quantity  $\tau_i$  is a constant for the corresponding  $i$ -process. Then the expression for calculating the equivalent frequency takes on the form [3]:

$$\nu_{eq} = \frac{w}{2\pi} \frac{c_i}{c_0} = \frac{w}{2\pi} \frac{c_i U_i}{k T_i}. \quad (4)$$

TABLE 1. Relaxation Characteristics of PES and PSF-N

Relax. transition	$U_i$ , kJ/mol		$T_i$ , °C*		$B_i$ , sec		$w$ , $10^2$ deg/sec	$c_i$		$\nu_{eq} \cdot 10^3$ , Hz	
	PES	PSF-N	PES	PSF-N	PES	PSF-N		PES	PSF-N	PES	PSF-N
$\beta$	47	38	-107	-112	$2,5 \cdot 10^{-16}$	$2,6 \cdot 10^{-14}$	6,3	3,6	4,5	2,8	2,3
$\beta_1$	64	52	-47	-48	$2,5 \cdot 10^{-16}$	$1,0 \cdot 10^{-13}$	4,7	5,0	6,5	1,5	1,1
$\beta_2$	73	72	27	47	$2,5 \cdot 10^{-14}$	$2,5 \cdot 10^{-13}$	4,7	6,7	6,8	1,0	1,1
$\beta_3$	109	94	152	133	$0,7 \cdot 10^{-14}$	$1,0 \cdot 10^{-13}$	3,8	9,7	11,0	0,5	0,5
$\alpha$	143	123	240	202	$5,0 \cdot 10^{-12}$	$5,0 \cdot 10^{-12}$	3,8	15	20	4,0	4,2

\*Relaxation transition temperatures for frequency of 1 Hz.

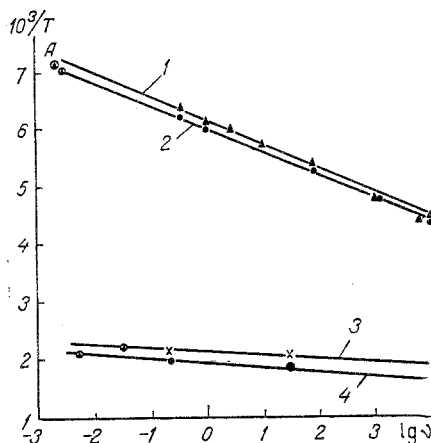


Fig. 3. Quantity  $1/T_i$  vs  $\log \nu$  for relaxation transitions: 1)  $\beta$  (PSF-N); 2)  $\beta$  (PES); 3)  $\alpha$  (PSF-N); 4)  $\alpha$  (PES).

The value of the constant  $c_i$  for fine-scale processes is equal to unity, and the value of the activation energy  $U_i$  is known. The equivalent mechanical frequency corresponding to a given scanning rate in our experiments is presented in Table 1 for the observed  $\beta$ -relaxation processes.

Low-temperature relaxation  $\beta$ -transitions in the internal stress spectra and the temperature dependence of specific heat for PSF-N and PES observed in the vitreous state with consideration of  $B_i$  and  $U_i$  values refer to fine-scale motions of macromolecules [9].

We will consider the possible molecular nature of the  $\beta$ -transitions. It was established in [8] that in aromatic polymers both in the presence and absence of link atoms in the basic chain (in the polysulfones considered here there are carbon, oxygen, and sulfur atoms) the  $\beta$ -transition is observed in one and the same temperature region. This means that rotation of phenylene groups is responsible for the  $\beta$ -relaxation. According to the data of [8], the  $\beta$ -relaxation mechanism is much more complex than simple rotation of the phenylene group. Thus, for example, introduction of link atoms would appear to facilitate rotation of  $C_6H_4$ -groups, but this does not occur in the case of  $\beta$ -relaxation. The temperature  $T_i$  of this transition does not decrease, but increases, while the vitrification temperature decreases due to a decrease in rigidity of the chains. The complexity of the  $\beta$ -process in polysulfones is also shown by the value of the coefficient  $B_i$ , which differs from the  $B_i = 1.6 \cdot 10^{-13}$  sec of linear carbochain polymers. Since the  $\beta_1$ -transition has a value of  $B_i$  similar to that of the  $\beta$ -transition, its mechanism is the same, but corresponds to rotation of the  $C_6H_4$ -group in a zone ordered amorphous phase. Therefore the activation energy (see Table 1) is greater than for the  $\beta$ -transition.

The existence of two amorphous structures in polysulfones can be explained by two types of microstructure in the macromolecule chains. For the one type the oxygen atom and the sulfone group  $SO_2$  are located on one side of parallel planes of the phenylene groups, while for the other, they are on opposite sides.

Upon rotation of the phenylene groups free rotational motion of link groups about the axis of the polymer chain is braked. The height of the rotation potential barriers for the oxygen atom is quite high, and higher still for the  $SO_2$ -group because of dipole-dipole forces developing between oxygen atoms of neighboring chains. The relaxation transition is characterized by values of  $B_i = 2.5 \cdot 10^{-14}$  for PES, and is probably related to thawing of rotational

motions of the link oxygen atom over valent cones. In view of the reasons presented above, the higher temperature  $\beta_3$ -transition can be related to a rotating  $\text{SO}_2$ -group. Thus, as rotations of phenylene groups ( $\beta$ - and  $\beta_1$ -processes), oxygen link atoms ( $\beta_2$ -processes), and  $\text{SO}_2$ -sulfone groups (the  $\beta_3$ -process) are enabled with increase in temperature new rotational degrees of freedom producing a contribution  $\Delta C_p$  to specific heat of polysulfones are enabled (Fig. 1, curves 1, 2).

The identical nature of the relaxation processes studied by thermophysical and mechanical methods is confirmed by the fact that results of thermophysical experiments fit well on the curve  $1/T = f(\lg \nu)$ , can be confirmed further by the following calculation, for example, of the most intense PSF-N-transition. We will use Eq. (3), transforming it to the form

$$T_i = \frac{U_i}{2,3k} \left( \lg \frac{c_i}{2\pi\nu_{\text{eq}}B_i} \right)^{-1}. \quad (5)$$

The temperature of the  $\beta$ -transition ( $T_p$ ) obtained with this expression is 143 K. The temperature of the maximum on the experimental curve (Fig. 1, curve 2) is equal to 148 K.

We see that the calculated and experimental values of the  $\beta$ -transition temperature are in good agreement, which indicates the single nature and identical timespans of the structural and mechanical relaxation processes. This is also confirmed by the results of Fig. 3, where the point A corresponds to thermophysical measurements. It is evident that this point fits well on the experimental dependence of  $1/T_i$  on  $\log \nu$ . The  $\alpha$ -relaxation process is characterized by a dependence of activation energy  $U_\alpha$  on temperature. Such a dependence is expressed by the Fulcher-Fogel-Tamman equation

$$U_\alpha = U_\infty / (1 - T_0/T). \quad (6)$$

In this case the constant  $c_0$  in the expression for calculating the equivalent frequency, Eq. (4), can be calculated with the expression

$$c_0 = \frac{kT_\alpha^2}{U_\alpha} \left[ 1 - \frac{T_\alpha}{U_\alpha} \left( \frac{dU}{dT} \right)_{T=T_\alpha} \right]^{-1}. \quad (7)$$

In accordance with Eq. (6)

$$\frac{T_\alpha}{U_\alpha} \left( \frac{dU}{dT} \right)_{T_\alpha} = - \frac{T_0}{T - T_0}.$$

Data on  $c_0$  and  $\nu_{\text{eq}}$  for PES and PSF-N  $\alpha$ -processes are also shown in Table 1, and in Fig. 3 (curves 3, 4) inverse temperature transitions are shown, as obtained from specific heat data (see Fig. 1).

Value of  $T_0$  for the PES and PSF-N  $\alpha$ -process were obtained from the Fulcher-Fogel-Tamman equation which comprised 431 K and 337 K respectively, together with  $U_\infty = 19$  kJ/mol and 20.3 kJ/mol. These values of the constants  $U_\infty$  and  $T_0$  permit calculation of the activation energy of the  $\alpha$ -process for various temperatures. Thus, for structural vitrification (Fig. 1) the PES  $\alpha$ -process activation energy is equal to 177 kJ/mol, with 123 kJ/mol for PSF-N. The  $U_\alpha$  values obtained agree well with those calculated with Eq. (5) with consideration of known values of  $T_i$  (obtained during experiment) and the values of  $\nu_{\text{eq}}$  found. Thus, for PSF-N  $U_\alpha$  from Eq. (5) is equal to 112 kJ/mol.

Thus, use of relaxation spectroscopy methods together with thermophysical methods permits study and explanation of the physical nature of relaxation processes in polysulfones, as well as prediction of their manifestation in various thermal and mechanical loading regimes.

#### NOTATION

$\lambda$ , thermal conductivity;  $C_p$ , specific heat;  $\tan \delta$ , tangent of mechanical loss angle;  $\Delta$ , damping decrement;  $U_i$ , activation energy;  $T_i$ , relaxation temperature;  $G'$ , dynamic shear modulus.

#### LITERATURE CITED

1. Polymer Encyclopedia [in Russian], Vol. 2, Moscow (1974), pp. 759-763.
2. N. I. Shut, T. G. Sichkar' and P. A. Voznyi, Composition Polymer Materials [in Russian], Vol. 24, Kiev (1985), pp. 18-24.

3. G. M. Bartenev, V. P. Dushenko, N. I. Shut, and M. V. Lazorenko, *Vys. Soed.*, A27, No. 2, 405-409 (1985).
4. V. V. Kharitonov, *Thermophysics of Polymers and Polymer Compositions* [in Russian], Minsk (1983).
5. G. M. Bartenev, M. V. Lazorenko, and N. I. Shut, *Vys. Soed.*, A27, No. 8, 1768-1772 (1985).
6. M. Baccaredda, E. Butta, V. S. de Petris Frosini, *J. Polym. Sci.*, 14, No. 5, pt. A-2, 1296-1299 (1976).
7. G. Allen, J. McCainsh, and G. M. Jeffes, *Polimer*, 12, No. 2, 85-100 (1971).
8. O. G. Nikol'skii, A. A. Askadskii, S. N. Salazkin, and G. L. Slonimskii, *Mechanics of Composition Materials* [in Russian], No. 6, Riga (1983), pp. 963-972.
9. G. M. Bartenev, *Structure and Relaxation Properties of Elastomers* [in Russian], Moscow (1982).

FEATURES OF HEAT TRANSFER IN A FLOW OF AIR IN A PLANE CHANNEL  
WITH UNSTAGGERED HALF-CYLINDRICAL PROJECTIONS

V. I. Velichko and V. A. Pronin

UDC 536.244

A study was made of local heat transfer in a flow of air with  $Re = (1,5-170) \cdot 10^3$ ,  $s_1/d = 1.27$ ;  $s_2/d = 5.33$ ; 3.04; 2.13. It was found that heat transfer is non-symmetrical on opposite sides of the channel.

In boiler design, great importance is attached to questions related to intensifying heat exchange and ensuring the reliable operation of convective heating surfaces. Experience accumulated in the operation of such surfaces shows the significant design, processing, and operational advantages of membrane panels used as convective and shielding elements. The studies [1-5] present data from investigations of local heat transfer, this data showing that to ensure reliable operation of a membrane structure, it is necessary to consider the effect of the nonuniform distribution of heat transfer on the temperature regime of the surface.

As in normal bundles, the pipes in such systems can be arranged in staggered or unstaggered fashion. The use of a given arrangement is dictated by the flow conditions and should be substantiated by special technicoeconomic calculations for each case. For example, it was noted in [6] that several design problems are encountered in achieving "economical" flue-gas velocities, but the authors also noted that these problems can be overcome by using unstaggered membrane bundles.

Calculations performed in [7] showed that an unstaggered bundle of tubes with solid fins is more efficient than a similar bundle of smooth tubes in the range  $Re_d \leq 10^4$ .

Along with this, as in the case of flow over a straight double ledge [8], flow and heat transfer may be nonsymmetrical under certain conditions in the case of a membrane surface with an unstaggered tube arrangement. These effects may have a significant influence on the temperature regime of the membrane panel.

These considerations interested us in taking a closer look at membrane heating surfaces with an unstaggered tube arrangement. To do this, we reconstructed the test section described in [7]: measurements were made only for an unstaggered arrangement of the projections, with a transverse relative step  $s_1/d = 1.27$  and three lengthwise steps  $s_2/d = 5.33$ , 3.04, and 2.13.

Heat transfer was measured on a flat wall and on semicylindrical calorimeters for both sides of the channel. Although realization of this reconstruction required many design

---

Moscow Power Institute. Translated from *Inzhenerno-Fizicheskii Zhurnal*, Vol. 53, No. 6, pp. 949-954, December, 1987. Original article submitted July 17, 1986.